

Mesoscopic conductance effects in $\text{In}_{1-x}\text{Mn}_x\text{As}$ structures

S. Lee¹, A. Trion¹, T. Schallenberg², H. Munezaka², and D. Natelson¹

¹Department of Physics and Astronomy, Rice University, Houston, TX 77005, USA and

²Imaging Science and Engineering Laboratory, Tokyo Institute of Technology, Yokohama, Kanagawa 226-8503, Japan
(Dated: June 23, 2021)

Quantum corrections to the electrical conduction of magnetic semiconductors are comparatively unexplored. We report measurements of time-dependent universal conductance fluctuations (TDUCF) and magnetic field dependent universal conductance fluctuations (MFUCF) in micron-scale structures fabricated from two different $\text{In}_{1-x}\text{Mn}_x\text{As}$ thin films. TDUCF and MFUCF increasing in magnitude with decreasing temperature are observed. At 4 K and below, TDUCF are suppressed at finite magnetic fields independent of field orientation.

PACS numbers: 73.23.+b, 73.50.-h, 72.70.+m, 73.20.Fz

Mesoscopic phenomena such as weak localization (WL), Aharonov-Bohm (AB) oscillations, and universal conductance fluctuations (UCF) are comparatively unexplored in ferromagnetic (FM) systems. In part, this is because of complicating effects such as the anisotropic magnetoresistance (AMR) and the interplay between conduction and FM domain structure. These materials are of fundamental interest since exchange correlations lead to collective degrees of freedom not present in normal metals. The interplay between FM order and coherence phenomena is also a topic of interest [1, 2]. A number of recent experiments have examined mesoscopic effects in FM systems [3, 4, 5, 6, 7, 8, 9, 10, 11, 12]. Recent measurements [13] in half-metallic CrO_2 suggest that coherence lengths of hundreds of nanometers are possible in ferromagnetic systems. The combination of electronic coherence and magnetism may also enable device technologies.

Ferromagnetic semiconductors (FSS) are an interesting material system to examine, since carrier-mediated spin exchange between Mn ions is thought to be the origin of the ferromagnetic phase [4, 15]. Two of the most studied FS systems [16] are $\text{Ga}_{1-x}\text{Mn}_x\text{As}$ and its close relative $\text{In}_{1-x}\text{Mn}_x\text{As}$. In these materials [17], one can achieve metallic conduction with ferromagnetic ordering at low temperatures with optimal doping, $x \approx 0.03-0.08$.

In this paper, we examine UCF in FM $\text{In}_{1-x}\text{Mn}_x\text{As}$ thin films. We perform both time-dependent UCF (TDUCF) and magnetic field-dependent UCF (MFUCF) measurements in Hall bars patterned from two different wafers at temperatures down to 2 K and magnetic fields, B , up to 9 T, oriented both along the current direction and perpendicular to the plane of the patterned FS film. For $T > 4$ K, the TDUCF are nearly independent of B . At lower temperatures, the TDUCF noise power decreases by roughly a factor of four as B is raised above zero. The magnitude and B dependence of the TDUCF are independent of the field orientation, suggesting that orbital effects are not the source of the noise reduction. The MFUCF data allow an order of magnitude estimate of the coherence length at 2 K of ≈ 50 nm. The magnitudes of the TDUCF and MFUCF are compared and discussed, as are their temperature dependence and the

TABLE I: Parameters for both $\text{In}_{1-x}\text{Mn}_x\text{As}$ samples used in the experiments. Resistivity, carrier density, and mobility are calculated from the sample resistance and the Hall resistance measured at 300 K, 3 T. All samples have wires of width 6.5 μm and thickness is 20 nm, and composed of six segments with length of 40 μm each.

Sample	x	T_c [K]	ρ [cm]	p_v [cm^{-3}]	μ [cm^2/Vs]
# 1	0.058	47	$14.2 \cdot 10^3$	$1.87 \cdot 10^{20}$	2.34
# 2	0.045	27	$11.2 \cdot 10^3$	$1.90 \cdot 10^{20}$	2.94

nature of the low temperature fluctuations that lead to the noise.

Provided films were grown on (100) GaAs wafers by molecular beam epitaxy (MBE), starting with highly resistive 500 nm AlSb buffer layers grown at a substrate temperature of 560 C with a growth rate of 0.9 $\mu\text{m}/\text{h}$. Then, 20 nm $\text{In}_{1-x}\text{Mn}_x\text{As}$ films were deposited at a substrate temperature of 200 C and with a V/III flux ratio, $r = 3:4$. Mn concentration was kept $< 6\%$ in order to avoid the formation of MnAs second phase. Details of the MBE process are reported in a recent separate paper [18]. Prepared in this manner, the magnetic easy axis of the $\text{In}_{1-x}\text{Mn}_x\text{As}$ is along the growth direction.

Two different films were used to fabricate identically shaped wire samples patterned by electron beam lithography. A 1 keV Ar^+ ion beam was used to sputter etch the extraneous film material. AFM measurements show that the widths of the wires and the narrow parts of leads were 6.5 μm , and the center to center distances between consecutive leads were 40 μm . Table I shows the specifications of the two samples. The resistivities for the processed material are several times higher than for the bulk films (3-5 $\text{m}\Omega\text{-cm}$). This suggests that the etching damages even the "unexposed" semiconductor, though the magnetic properties appear essentially unaffected by the etching.

All measurements were performed in a ^4He cryostat, with the magnetic field either normal to the plane of the wire ("perpendicular") or along the wire axis ("parallel"). Longitudinal and Hall resistances were measured using conventional ac four-terminal lock-in methods, whereas TDUCF and MFUCF were measured us-

ing an ac voltage-bridge technique [20]. Excitations were restricted to levels that avoided Joule self-heating of the carriers, checked by comparing temperature dependences of measurements at different drive amplitudes. This requirement sets the lower temperature limit of the noise measurements.

Typical $\text{In}_{1-x}\text{Mn}_x\text{As}$ is paramagnetic above its Curie temperature, T_c , which is between 10 and 100 K depending on Mn concentration, substrate temperature, and resulting disorder during the growth process [18]. Fig. 1 (a) and (b) show the temperature dependence of the longitudinal and Hall resistance, respectively, for sample # 1 whereas Fig. 1 (c) and (d) are for sample # 2. The resistance peaks at T_c between 30–50 K while cooling, and the transition is clear in the Hall resistance, which exhibits ferromagnetic hysteresis for $T < T_c$ (grey lines). This is more pronounced as T is further reduced (black lines). In the TDUCF and MFUCF measurements, T is well below T_c .

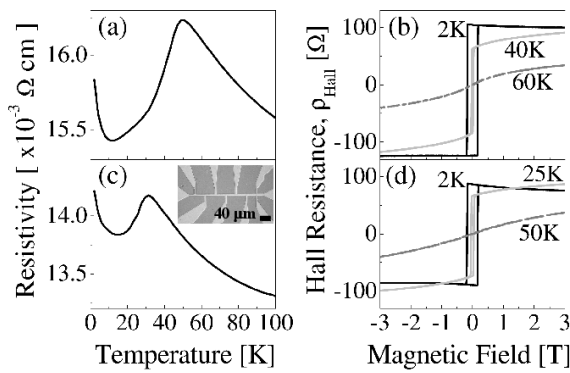


FIG. 1: (a) Resistivity of sample # 1 shows its Curie temperature around 50 K. (b) Hall resistance measurement for sample # 1 at 60 (dashed line), 40 (grey line), and 2 K (black line) showing magnetic hysteresis upon cooling, as expected for the paramagnetic to ferromagnetic transition. (c) Resistivity for sample # 2 shows its Curie temperature lies \sim 30 K. (d) Hall resistance for sample # 2 at 50 (dashed line), 25 (grey line) and 2 K (black line). Inset: SEM image of etched sample.

Figure 2 shows the results of the TDUCF noise power, $S_R(T)$, measurements on the two samples. The frequency dependence of the raw voltage noise power [19] is well described as $1=f$. The parameter plotted is the coefficient of the $1=f$ dependence, normalized by drive current and sample resistance to units of 1/Hz. The noise floor of the measurement setup has been subtracted from these data. Closed (open) symbols indicate the perpendicular (parallel) field configuration. The increase of noise power as T is decreased is a unique, distinguishing feature expected in TDUCF, and results from the growth of the coherence length, L [9].

The inset to Fig. 2 (b) shows $S_R(T)$ at zero-field and $B = 3$ T for sample # 2; the same trends are seen in sample # 1. Above \sim 5 K at $B = 0$ as well as over the whole temperature range for the high field data, the noise power varies approximately as $T^{-0.5}$. In the low

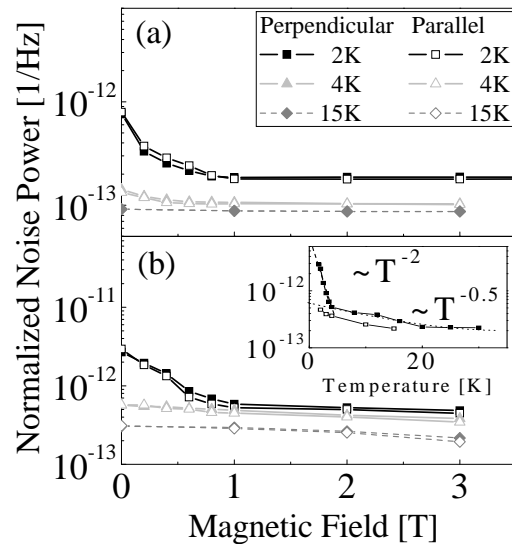


FIG. 2: Normalized noise powers as a function of external magnetic field for (a) sample # 1, and (b) sample # 2 are shown at three different temperatures, 2 K (solid black lines), 4 K (solid light grey lines), and 15 K (dashed grey lines). Closed symbols are for perpendicular configuration, and open symbols are for parallel configuration. Inset shows the temperature dependence of noise power for sample # 2 at 0 T (solid symbol) and 3 T (open symbol). Error bars are not shown in these plots because they are comparable to the symbol size.

temperature limit, the noise power scales approximately as T^{-2} . Both of these dependences differ from the temperature dependence seen in nonmagnetic metals. In normal metals, the expected [21, 22] $S_R(T) \sim n(T)L_{\min}^2L^2$, where $n(T)$ is the density of thermally active fluctuators, L_{\min} is the smaller of L or $L_T \sim D k_B T$, the thermal length. For standard two-level fluctuators, $n(T) \sim T^{-1}$, and in typical metals, $L_T < L$, implying that $S_R \sim L^2$. The unusual temperature dependence seen in FS samples therefore suggest either (a) the fluctuators have an unusual energy distribution despite having the usual distribution of relaxation times that gives $S_R \sim 1/f$; or (b) the dephasing mechanism for holes in this material is unconventional.

In normal metals, the field-dependent suppression of the cooperon contribution to the TDUCF provides a means of quantitatively assessing L without recourse to these assumptions about the distribution of fluctuators [23]. In a ferromagnetic system with broken time-reversal symmetry, no such decrease in noise power is expected, since the cooperon contribution is likely already suppressed. This was borne out in permalloy wires [9]. In contrast, $S_R(B)$ in the $\text{In}_{1-x}\text{Mn}_x\text{As}$ system is striking at low temperatures, and strongly implies that the dominant source of TDUCF is coherent scattering of carriers off fluctuating magnetic disorder. Qualitatively similar effects have been seen at millikelvin temperatures in magnetic semiconductors that are spin glasses [3]. Above 5 K, S_R is essentially independent of B , as seen in the permalloy experiments [9]. However, as T is reduced

below 5 K, S_R acquires a field dependence for $\beta j < 1$ T. For both samples, $S_R(B = 0 \text{ T})$ becomes almost four times larger than $S_R(B = 1 \text{ T})$ at 2 K. As shown in Fig. 2, this field dependence is approximately independent of field orientation. This is consistent with a field-driven Zeeman suppression of the fluctuations that cause the noise, rather than an orbital coherence effect as in TDUCF in normal metals.

UCF as a function of magnetic field (MFUCF) rather than time provide a consistency check on the idea that Zeeman rather than orbital physics is relevant to $S_R(B)$. Since Aharonov-Bohm shifting of phases of electronic trajectories is equivalent to altering the impurity configuration [4], sweeping B leads to sample-specific, reproducible MFUCF within a coherent volume. The correlation field scale of the fluctuations, B_c , is related to the size of typical coherent trajectories via the flux quantum, h/e . Figure 3 (a) shows MFUCF for sample # 1 in three different temperatures 2, 4, and 10 K from $B = -9 \text{ T}$ to 9 T when sample lies in perpendicular configuration. The symmetry in B about $B = 0$ outside of the hysteretic portion of the conduction response confirms that these fluctuations are real. Qualitatively similar MFUCF occur in sample # 2. Note that the MFUCF reproduce when B is swept up and back. We assume a quasi-2d response, $B_c L^2 = h/e$, and check for consistency. While far more fluctuations are required for a quantitative estimate, Fig. 3 (b) suggests that B_c at 2 K is on the order of 2 T, which would imply coherence length, $L = 50 \text{ nm}$, larger than sample thickness as required for self-consistency. A truly quasi-2d sample would exhibit weaker fluctuations in the parallel configuration, and this is consistent with Figs. 3 (c) and (d). The MFUCF variance varied like T^{-4} dependence below 4 K, stronger than the TDUCF variance, though statistics are poor because the apparent field scale of the MFUCF is so large.

The microscopic origins of the TDUCF remain a subject for further investigation. One possibility is that the fluctuations are associated with Mn spins, perhaps at the edges of the sample, not fully participating in the bulk FM order of the system. Coherent scattering of slowly fluctuating local magnetization could cause TDUCF, as in the spin glass case mentioned previously [3]. At sufficiently large B those moments would be saturated, removing that source of fluctuations. This does not, how-

ever, explain the particular forms of $S_R(B; T)$, and the similarity in temperature dependence in the low T limit to that seen previously in perm alloy wires.

In summary, we have examined quantum corrections to the electronic conduction in InMnAs nanostructures. The observed dependences of TDUCF and MFUCF on temperature and magnetic field place constraints on the noise and decoherence processes at work in this material. InMnAs is another rich laboratory in which to examine quantum coherence in the presence of ferromagnetism, physics that may enable future device technologies.

This work was supported by DOE grant DE-FG03-01ER45946/A001 and the David and Lucille Packard

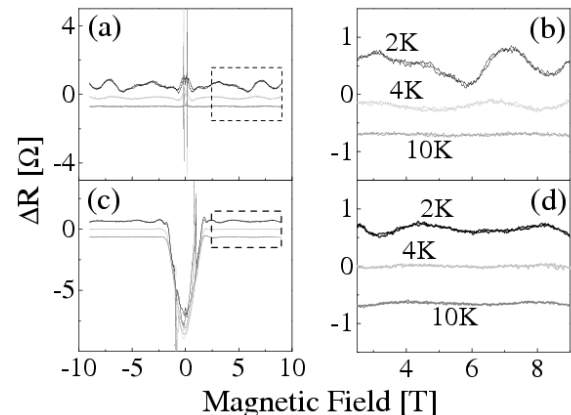


FIG. 3: MFUCF measurements of $R - R(B) - R(B = 0)$ for sample # 1 in (a) perpendicular and (c) parallel configurations were done using the four-terminal bridge technique. Measurements were performed at three different temperatures 2, 4, and 10 K for the field span of -9 T to $+9 \text{ T}$. The curves are offset for clarity and a smooth background magnetoresistance due to imperfect symmetry between the two sides of the bridge is subtracted from each curve. (b) and (d) are zoomed-in version for the marked area in (a) and (c), respectively.

Foundation. TS and HM acknowledge support in part by Grant-in-Aid for Scientific Research from MEXT and JSPS (No. 14076210 and No. 17206002), and by the NSF-IT program (DMR-0325474) in collaboration with Rice University.

[1] K. Hong and N. Giordano, Phys. Rev. B 51, 9855 (1995).
 [2] G. Tatara and H. Fukuyama, Phys. Rev. Lett. 78, 3773 (1997).
 [3] J. Jaroszynski, J. Wrobel, M. Sawicki, E. Kaminska, T. Skoskiewicz, G. Karczewski, T. Wojtowicz, A. Piotrowska, J. Kossut, and T. Dietl, Phys. Rev. Lett. 75, 3170 (1995).
 [4] M. Aprili, J. Lesueur, L. Mouchelin, and P. Nedelac, Sol. Stat. Comm. 102, 41 (1997).
 [5] J. Aumentado and V. Chandrasekhar, Physica B 284-

288, 1742 (2000).
 [6] V. K. Dugaev, P. Bruno, and J. Bamas, Phys. Rev. B 64, 144423 (2001).
 [7] S. Kasai, T. Niigama, E. Saitoh, and H. Miyajima, Appl. Phys. Lett. 81, 316 (2002).
 [8] S. Kasai, E. Saitoh, and H. Miyajima, J. Appl. Phys. 93, 8427 (2003).
 [9] S. Lee, A. Trion, and D. Natelson, Phys. Rev. B 70, 212407 (2004).
 [10] Y. G. Wei, X. Y. Liu, L. Y. Zhang, and D. D. Avidovic,

Phys. Rev. Lett. 96, 146803 (2006).

- [1] K. Wagner, D. Neumaier, M. Reinwald, W. Wegscheider, and D. Weiss, Phys. Rev. Lett. 97, 056803 (2006).
- [2] L. Vila, R. Giraud, L. Thevenard, A. Lemaitre, F. Pierre, J. Dubouleur, D. Mailly, B. Barbara, and G. Faini, cond-mat/0609410 (2006).
- [3] R. S. Keizer, S. T. B. Goennenwein, T. M. Klapwijk, G. Miao, X. Yao, and A. Gupta, Nature 439, 825 (2006).
- [4] T. Dietl, A. Haury, and Y. M. Dubigne, Phys. Rev. B 55, R3347 (1997).
- [5] J. König, H. H. Lin, and A. H. MacDonald, Phys. Rev. Lett. 84, 5628 (2000).
- [6] H. Muneoka, in Concepts in Spin Electronics, edited by S. Mookawa (Oxford Science Publications, Oxford, 2006).
- [7] Y. Iye, A. Ojima, A. Endo, S. Katsumoto, F. Matsukura, A. Shen, H. Ohno, and H. Muneoka, Mat. Sci. Eng. B 63, 88-95 (1999).
- [8] T. Schallenberg and H. Muneoka, Appl. Phys. Lett. 89, 042507 (2006).
- [9] See EPAPS Document No. *** for detailed sample parameters, representative WL and noise data, temperature dependences of TDF, and calculations related to the noise magnitude. A direct link to this document may be found in the online article's HTML reference section. The document may also be reached via the EPAPS homepage (<http://www.aip.org/pubservs/epaps.html>) or from <ftp://ftp.aip.org> in the directory /epaps/. See the EPAPS homepage for more information.
- [20] J. H. Scofield, Rev. Sci. Instr. 58, 985 (1987).
- [21] S. Feng, P. A. Lee, and A. D. Stone, Phys. Rev. Lett. 56, 1960 (1986).
- [22] N. O. Birge, B. G. Orling, and W. H. Haemmerle, Phys. Rev. Lett. 62, 195 (1989).
- [23] A. D. Stone, Phys. Rev. B 39, 10736 (1989).
- [24] P. A. Lee, A. Douglas Stone, and H. Fukuyama, Phys. Rev. B 35, 1039 (1987).
- [25] T. Dietl, H. Ohno, and F. Matsukura, Phys. Rev. B 63, 195205 (2001).

Due to space limitations in the main manuscript, here we show two supplemental figures that provide further information about the experiments.

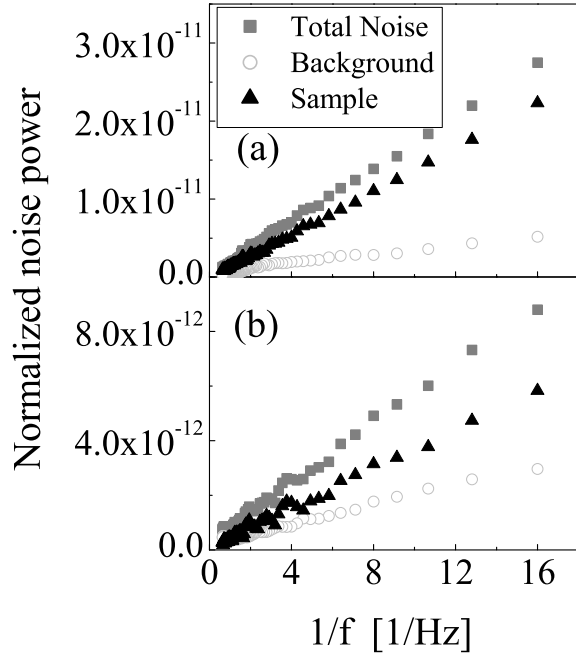


FIG. 4: Normalized raw noise data for sample # 1, for (a) $T = 2 \text{ K}$, $B = 0 \text{ T}$, and (b) $T = 15 \text{ K}$, $B = 3 \text{ T}$, with the field oriented perpendicular to the plane of the sample.

Figure 4 shows the measured noise power from the in-phase channel of the lock-in amplifier (squares), the measured system background noise from the out-of-phase channel of the lock-in (circles), and their difference (triangles), for the high noise (a) and low noise (b) limits of the experiment, plotted versus $1/f$. The noise signals in V^2 corrected for amplifier gain have been normalized

by $(I_{\text{dir}}R)^2$, where I_{dir} is the drive current used for the measurement. Note that even at 15 K and 3 T, the noise signal is readily detectable above the background noise of the circuit.

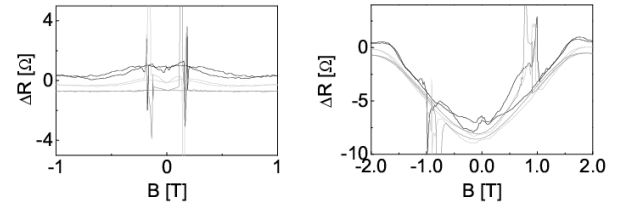


FIG. 5: Rescaled plots of the data from Fig. 3 of the main paper, showing the hysteretic region of the magnetoresistance data for (left) B perpendicular to the sample plane, and (right) B along the direction of the sample. Top to bottom at high fields, the data are 2 K, 4 K, and 10 K.

Figure 5 shows rescaled plots of the low-field regions of the magnetoresistance data from Fig. 3 of the paper, for both field orientations. Note that these data were taken using the same four-terminal bridge method as the noise data. In an ideal sample configuration, the two sides of the bridge would be exactly symmetrical, and bulk magnetoresistive effects such as the anisotropic magnetoresistance would be perfectly nulled away. The low-field regions shown here demonstrate that the actual samples are slightly unsymmetrical, such that the field-driven reorientation of the sample magnetization does not happen uniformly across the whole sample. As a result, there is some hysteresis seen in these plots as the magnetization is coerced at slightly different fields in the two halves of the sample. In the parallel field configuration, the main effect seen is the un-nulled portion of the anisotropic magnetoresistance, as M is coerced away from the perpendicular direction favored by crystallographic anisotropy, and into the direction of current flow.